JOURNAL OF OPTOELECTRONICS AND ADVANCED MATERIALS Vol. 10, No. 10, October 2008, p. 2522 - 2527

The influence of nonlinear polarization rotation of SOA on the output pulse of harmonic mode-locked fiber ring laser

GUANG-YU JIANG*, YAN HUANG, YONG-QING GONG
College of Automation, Nanchang Hangkong University, Nanchang 330063, China

Actively mode-locked fiber lasers based on the semiconductor optical amplifier(SOA),which are capable of generating ultra-short pulse train with high quality and high repetition rates,have received considerable attention.After considering the nonlinear polarization rotation in the SOA, a theoretical model of the harmonic mode-locked fiber ring laser based on SOA has been established. Using this model, for the different bias currents of the SOA, the influence of the nonlinear polarization rotation in the SOA on the shape, peak power, and pulse width of the pulse output from the harmonic mode-locked fiber ring laser has been investigated theoretically. Numerical results show that the mode-locked pulses whose peak power and pulse width are 0.16mW and 6ps for the low currents, 0.56mW and 19.8ps for the high currents respectively, can be obtained for the harmonic mode-locked fiber ring laser.

(Received March 3, 2008; accepted August 14, 2008)

Keywords: Optical communication; Semiconductor optical amplifier(SOA); Nonlinear polarization rotation, Harmonic mode-locking

1. Introduction

Light sources capable of generating stable short pulse trains are one of the key components for the implementation of high speed wavelength division multiplexing (WDM) and optical time division multiplexing (OTDM) transmission systems[1].Among the various means of producing optical pulse train, an actively mode-locked fiber laser is one of the most practical and efficient methods for the generation of wavelength tunable, transform-limited, high quality picosecond optical pulses at high repetition rates with relatively low amplitude noise and timing jitter. The harmonically mode-locked erbium-doped fiber laser (EDFL) is very attractive as a high repetition rate pulse source. The EDFL requires the configuration of long cavity length to obtain sufficient gain from the EDFA [2, 3], which results in the instability of the output pulse train, from even small environmental perturbation, such as thermal fluctuations and acoustic vibrations that affect the fiber laser. To overcome the sensitivity to environmental perturbations, the fiber ring lasers incorporating the semiconductor optical amplifier (SOA) as a gain medium have been reported, and the rational harmonic mode-locking technique has been investigated, which produces an optical pulse train with high repetition rates. The numerical model was developed which mostly aimed at investigating and understanding the operation of self-phase modulation (*SPM*) [4], cross-gain modulation (*XGM*) [5,6], cross-phase modulation (*XPM*)[7], four-wave mixing (*FWM*)[8] in the SOA on the actively mode-locked fiber ring laser. The nonlinear polarization rotation in the SOA has received considerable attention in recent years. X.Yang, et al. reported on the realization of a passively mode-locked ring-laser based on nonlinear polarization rotation in the SOA as the mode-locking mechanism and a linear polarizer.The ring cavity generates pulses with duration below *800fs*(FWHM) at a repetition rate of *14Mhz*[9].However, the influence of nonlinear polarization rotation in the SOA on the generated pulses of the actively mode-locked fiber ring laser was scarcely referred in both theoretically and experimentally.In this paper, a theoretical model of the harmonic mode-locked fiber ring laser based on the nonlinear polarization rotation in the SOA has been established and the influence of the nonlinear polarization rotation in the SOA on the shape, peak power, and pulse width of the pulse output from the harmonic mode-locked fiber ring laser has been investigated for the different bias currents of the SOA. This result will be helpful for designing and researching into the harmonic mode-locked fiber ring laser based on the SOA.

2. Theory

The schematic diagram of the harmonic mode-locked fiber ring laser based on the nonlinear polarization rotation in the SOA, is shown in Fig. 1, the harmonic mode-locked fiber ring laser consists of the SOA, the polarization controller (*PC*), the tunable filter and the polarizer. The SOA is used to provide the necessary gain and as the mode locker, the *PC* is used to control the optical polarization state, and the Faraday optical isolators ensure a unidirectional cavity. In order to obtain stable pulse series in the cavity, the modulating frequency (f_1) of the modulator should be nearly integral times the fundamental frequency (f_0) of the cavity, that is to say, $f_1=Nf_0$ (N is a positive integer). So the nth-order harmonic mode-locking pulse series are achieved and output from the second OC_2

with ratio of *90:10*, the repetition rate (f_0) of mode-locked pulse is the same as the modulating frequency.

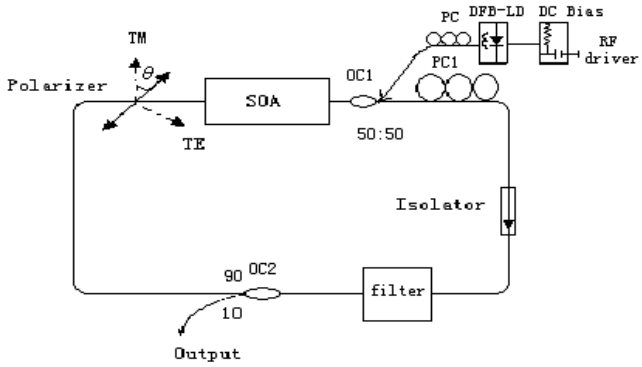

Fig. 1. Schematic diagram of harmonic mode-locked based on the SOA.

The model is based on the decomposition of the incoming arbitrarily polarized electric field into a component parallel (*TE* mode) to the layers in the active waveguide and a perpendicular component (*TM* mode). These two polarization directions are along the principal axes that diagonalize the wave propagation in the SOA. In practice, apart from their indirect interaction through the carrier dynamics in the device, these two polarizations propagate independently from each other. In this paper, the model is developed to describe the polarization behavior up to speeds of a few tens of gigahertz, so the relatively simple propagation and rate equations are adopted, namely without necessity of taking into account the ultrafast intraband relaxation dynamics. The propagation equations for the *TE* and *TM* modes, are expressed as [10-12]

$$(\frac{\partial}{\partial t}+\upsilon_g^{TE}\frac{\partial}{\partial z})\mathrm{A}^{TE}(z,t)=\frac{1}{2}\Gamma^{TE}(1+i\alpha^{TE})g^{TE}(z,t)\mathrm{A}^{TE}(z,t)-\frac{1}{2}\alpha_{\mathrm{int}}^{TE}\mathrm{A}^{TE}(z,t) \tag{1}$$

$$(\frac{\partial}{\partial t}+\upsilon_g^{TM}\frac{\partial}{\partial z})\mathrm{A}^{TM}(z,t)=\frac{1}{2}\Gamma^{TM}(1+i\alpha^{TM})g^{TM}(z,t)\mathrm{A}^{TM}(z,t)-\frac{1}{2}\alpha_{\mathrm{int}}^{TM}\mathrm{A}^{TM}(z,t) \tag{2}$$

Here, the *TE* and *TM* donate the transverse electric field component and the transverse magnetic field component, respectively. $A(z,t)$ is the weakly time and space-dependent complex envelope of the optical field, v_g the corresponding group velocity taken at the central frequency of the wave, Γ the confinement factor, $g(z,t)$ the gain function, α the phase-modulation parameter, and a_{int} the modal loss. The envelopes for each polarization are

$$\mathrm{A}^{TE}(z,t)=\sqrt{S^{TE}(z,t)}e^{i\phi^{TE}(z,t)}$$
$$\mathrm{A}^{TM}(z,t)=\sqrt{S^{TM}(z,t)}e^{i\phi^{TM}(z,t)} \tag{3}$$

where $S(z,t)$ and ϕ (z,t) are respectively the photon numbers and the phases for the *TE* and *TM* components. The gain $g(z,t)$ for *TE* and *TM* polarization ,is given by

$$g^{TE}(z,t)=\xi^{TE}\left[n_c(z,t)+n_x(z,t)-N_0\right] \tag{4a}$$

$$g^{TM}(z,t)=\xi^{TM}\left[n_c(z,t)+n_y(z,t)-N_0\right] \tag{4b}$$

Where $\xi^{TE/EM}$ is the gain coefficient for the *TE* and *TM* mode, N_0 is the total number of electronic states involved in the optical transition.$n_x(z,t)$ is the number of electrons in the conduction band, $n_x(z,t)$ and $n_y(z,t)$ are the number of holes involved in the *x* and *y* transitions. In cases of high intensity optical beams, one should correct $\xi^{TE/TM}$ for saturation due to the carrier heating according to

$$\xi^{TE}=\frac{\xi_0^{TE}}{1+\varepsilon S^{TE}} \qquad \xi^{TM}=\frac{\xi_0^{TM}}{1+\varepsilon S^{TM}} \tag{5}$$

where $\xi_0^{TE/TM}$ is differential gain coefficient in a small-signal, ε is nonlinear gain coefficient and $S^{TE/TM}$ is the average photon density. Assuming that the total number of holes is equal to the number of electrons

$$n_c(z,t)=n_x(z,t)+n_y(z,t) \tag{6}$$

and substitute this into (4) , g^{TE} *and* g^{TM} can be expressed as

$$g^{TE}(z,t)=\xi^{TE}[2n_x(z,t)+n_y(z,t)-N_0] \tag{7a}$$

$$g^{TM}(z,t)=\xi^{TM}[2n_y(z,t)+n_x(z,t)-N_0] \tag{7b}$$

The rate-equation for $n_x(z,t)$ and $n_y(z,t)$ can be written as

$$\frac{\partial n_x(z,t)}{\partial t}=-\frac{n_x(z,t)-\bar{n}_x}{T_1}-\frac{n_x(z,t)-fn_y(z,t)}{T_2}-g^{TE}(z,t)S^{TE}(z,t) \tag{8a}$$

$$\frac{\partial n_y(z,t)}{\partial t}=-\frac{n_y(z,t)-\bar{n}_y}{T_1}-\frac{n_y(z,t)-fn_x(z,t)}{T_2}-g^{TM}(z,t)S^{TM}(z,t) \tag{8b}$$

where $\bar{n}_x$ and $\bar{n}_y$ are the respective equilibrium values determined by the adopted pump current as will be

discussed below, T_1 is the electron–hole recombination time, and T_2 is the inter-hole relaxation time. The last terms in the right-hand sides of Eq.(8) account for the stimulated recombinations. It should be noted that the inter-hole relaxation time T_2 (~100 fs) is much shorter than the electron hole recombination time T_1 (~500 ps). The two populations will be clamped tightly together, i.e.,

$$n_x(z,t) = fn_y(z,t) \tag{9}$$

In case of unstrained bulk material, the gain will be isotropic and $f=1$. In case of tensile strain, *TM* gain will be larger than *TE*, i.e., $f<1$. n_x and n_y are the respective equilibrium values given by

$$\bar{n}_x = \frac{\overline{nf}}{1+f} \qquad \bar{n}_y = \frac{\bar{n}}{1+f} \tag{10}$$

where $\bar{n} = \frac{I}{e}T_1$, and I is the electric current and e is the electric unit charge. In Eqs.(9)–(10), f expresses the magnitude of the anisotropy.

The optical power for each mode is related to the the photon numbers through the following equation

$$S^{TE/TM} = \frac{P^{TE/TM}}{\hbar\omega}\frac{L}{\upsilon_g^{TE/TM}} \tag{11}$$

where $\hbar$ is Planck's constant, ω is the optical frequency, and L is the active length of the SOA. The differential equations that describe the space-varied intensities and phases of *TE* and *TM* modes, are given by

$$\frac{\partial S^{TE}(z,t)}{\partial z} = \left[\Gamma^{TE} g^{TE}(z,t) - \alpha_{\text{int}}\right] S^{TE}(z,t) \tag{12a}$$

$$\frac{\partial S^{TM}(z,t)}{\partial z} = \left[\Gamma^{TM} g^{TM}(z,t) - \alpha_{\text{int}}\right] S^{TM}(z,t) \tag{12b}$$

$$\frac{\partial \phi^{TE}(z,t)}{\partial z} = \frac{1}{2}\frac{\alpha^{TE}\Gamma^{TE} g^{TE}(z,t)}{\upsilon_g^{TE}} \tag{13a}$$

$$\frac{\partial \phi^{TM}(z,t)}{\partial z} = \frac{1}{2}\frac{\alpha^{TM}\Gamma^{TM} g^{TM}(z,t)}{\upsilon_g^{TM}} \tag{13b}$$

The output pusle after the SOA is elliptically polarized due to the difference in phase delay of *TE*-*TM* components, but it is linearized by the polarization controller after the SOA. So the output optical field can be written as

$$A_{out} = \sqrt{S_{out}^{TE}}\cdot e^{(i\phi^{TE})} + \sqrt{S_{out}^{TM}}\cdot e^{(i\phi^{TM})} \tag{14}$$

where

$$\mathrm{S}_{\text{out}}^{\text{TE}} = \mathrm{S}_{\text{in}}\cos^2\theta\cdot \mathrm{e}^{(\Gamma^{\text{TE}}\mathrm{g}^{\text{TE}}-\alpha_{\text{int}}^{\text{TE}})(\mathrm{L}/\upsilon_{\mathrm{g}}^{\text{TE}})},$$
$$\mathrm{S}_{\text{out}}^{\text{TM}} = \mathrm{S}_{\text{in}}\sin^2\theta\cdot \mathrm{e}^{(\Gamma^{\text{TM}}\mathrm{g}^{\text{TM}}-\alpha_{\text{int}}^{\text{TM}})(\mathrm{L}/\upsilon_{\mathrm{g}}^{\text{TM}})}$$

S_{in} represents the intensity of polarized electric field at the SOA input; θ is the angle between the polarized electric field and *TE* axes and can be adjusted by the polarizer.

The transfer function of the tunable filter, is expressed as [7]

$$T(\omega) = \exp\left[-\frac{(\omega-\delta\omega)^2}{2\Delta\omega_g^2}\right] \tag{15}$$

where $\delta\omega$ is the difference between the frequency of the optical pulse and central frequency of the filter, the relation between the $\Delta\omega_g$ and the *3dB* bandwidth of the filter, is written as

$$\Delta\omega_g = \frac{1}{2\sqrt{\ln 2}}\Delta\omega_{FWHM} \tag{16}$$

Based on Eqs.(1-16), the temporal shape of output pulse for a given input pulse passing though the SOA can be simulated numerically with forth-fifth order Rung-Kutta method. The obtained optical pulse is taken as the new incident pulse and repeats the above procedure. Only once the pulse realizes self-reproduction, the output optical pulse is the mode-locked optical pulse.

3. Results and discussion

Assuming that the sinusoidal wave with modulation frequency (f =2GHz) output from the gain switch *DFB-LD*. In the simulation, the other parameters used are

$\Gamma_{TE}=0.2, \Gamma_{TM}=0.14, a_{int}^{TE}=a_{int}^{TM}=0.27\mu m^{-1}, N_0=10^8, e=1.6\times10^{-19}C, V_g^{TE}=V_g^{TM}=100\mu m/ps, T_2=0.1ps, T_1=500ps, a^{TE}=a^{TM}=5$, $\xi_0^{TE}=7.0\times10^{-9}ps^{-1}$, $\xi_0^{TM}=6.5\times10^{-9}ps^{-1}$, $L=800\mu m, f=0.5$, $\theta=45^0, \varepsilon=10^{-7}$.

Fig.2 shows the output mode-locked pulse shape

versus the different bias currents of the SOA.The bias currents of the SOA are *102mA, 103mA, 104mA, 105mA, 106mA, 107mA, 108mA, 109mA, 110mA*,respectively in Fig.2 (a)-(i). It is visible in Fig.2 that when the bias current of the SOA is*102mA*, the output pulse width is the narrowest and the pulse shape is very symmetrical. With the increase of the bias currents of the SOA, the leading edge of the mode-locked pulse is steeper than the tailing edge, where the pulse distortion occurs, the pulse takes on asymmetry. This is due to the effect of the self-polarization rotation that the weak pedestal of the leading edge of the mode-locked pulse is suppressed; In contrast to this, the trailing edge of the output pulse has a long tail, which is caused by gain saturation difference between the *TE* and *TM* modes[12]; However, with increasing of the SOA bias currents, the pulse due to the saturation characteristic of SOA degenerates gradually without being provided sufficient gain. Fig.3 presents the peak power and pulse width for the different bias currents of the SOA. It is clear that, the final pulse width increases from *6* to *19.8ps* when the bias currents of the SOA are increased from *102* to *110mA*, while the mode-locked pulse peak power increases from *0.16* to *0.56mW* gradually. The reason is that, as the bias currents of the SOA increase, the carrier density increases gradually, and the peak power enhances; the gain difference between the *TE* and *TM* modes for high currents is further away from the initial value than that for low currents, which makes the pulse compression less efficient for the high currents than that for the low currents, the pulse width is widened gradually.

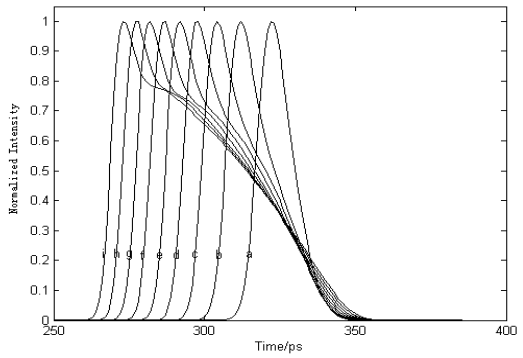

Fig. 2. Pulse shape at different bias currents of the SOA.

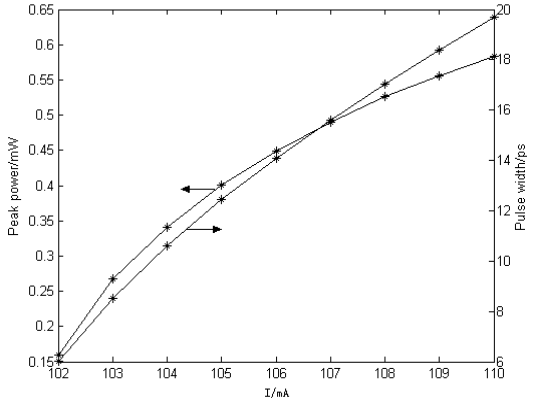

Fig. 3. Peak power and pulse width with the different bias currents of the SOA.

Fig .4 shows the peak power and pulse width of the output pulse as a function of the roundtrips at the different bias currents of the SOA.The bias currents of the SOA are *102mA (curve a), 103mA (curve b), 104mA (curve c), 105mA (curve d), 106mA (curve e), 107mA (curve f), 108mA (curve g), 109mA (curve h), 110mA (curve i)*, respectively. Here we observe that, the peak power of pulse enhances to its maximum value after its initial drop in the first several roundtrips. After about *1000* roundtrips, the pulse peak power remains approximately constant. While the corresponding pulse width takes on a rapid initial drop, followed by surging under the certain currents, finally even the pulse width becomes stable. This is caused by the incomplete recovery of gain and gain saturation difference of *TE* and *TM* modes. When the bias currents of the SOA increase gradually, the carrier intensity in the SOA increases, which leads to the peak power increase rapidly and the pulse width become narrower. After several thousands of roundtrips(>1000), the pulse width and peak power go to steady without maintaining the required gain.

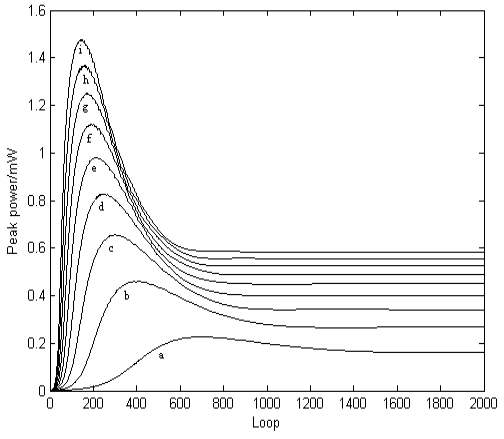

a

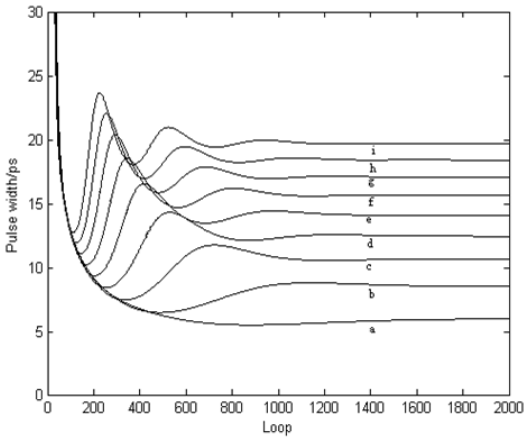

b

Fig. 4. Peak power and pulse width as a function of the roundtrips at different bias currents of the SOA.

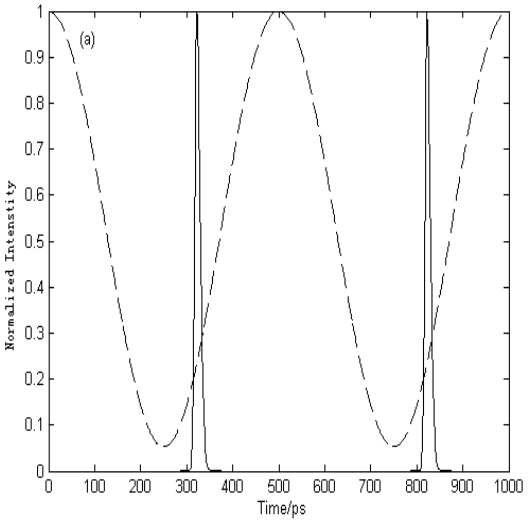

a

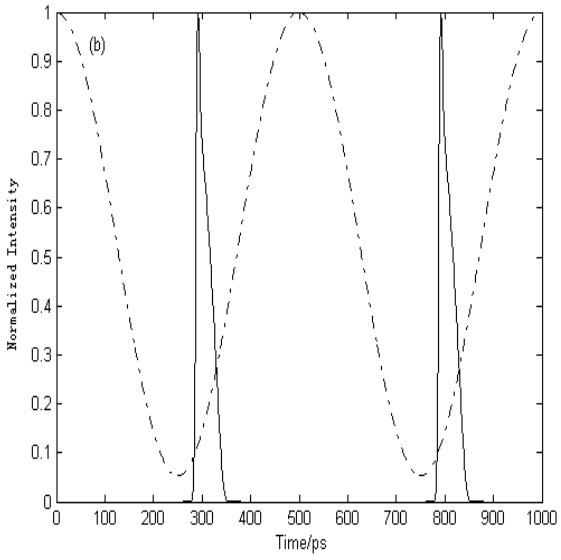

b

Fig. 5. Incident pulse and output pulse for the bias currents of the SOA (102mA and 106mA).

Fig.5 shows the incident pulse and output pulse for the bias currents of the SOA (*102mA and 106mA*, respectively). In Fig.5 (a) and (b), it can be seen that, for the low current, the output pulse width is much narrower, and the pulse shape symmetry is very good. When the bias current of the SOA is high, the nonlinear polarization rotation in the SOA is very strong, and the gain variety of the *TE* and *TM* modes is great, which lead to the pulse broadening and asymmetric.

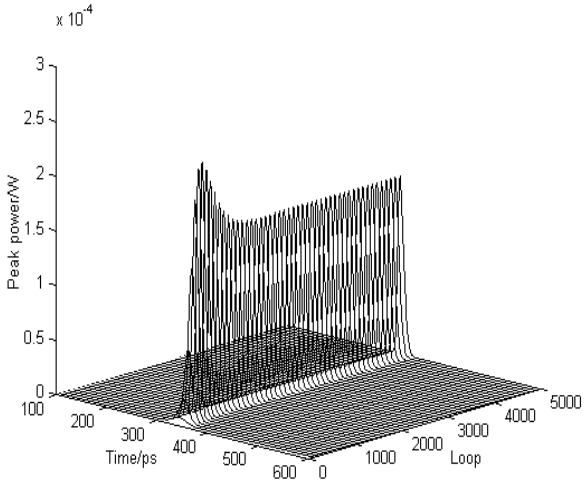

Fig. 6. Pulse evolution as a function of the number of roundtrips.

Fig. 6 shows the output pulse evolution at different roundtrips. When the bias current of the SOA is *102mA*. From this diagram, it can be shown that, for given conditions, the pulse has evolved into a stable shape, namely the pulse can realize self-reproductive after several thousands of roundtrips.

4. Conclusions

In conclusion, a theoretical model of the harmonic mode-locked fiber ring laser based on the nonlinear polarization rotation in the SOA has been established and investigated emphatically that, for the different bias currents of the SOA, the influence of the nonlinear polarization rotation in the SOA on the shape, peak power, and pulse width of the pulse output from the harmonic mode-locked fiber ring laser. By taking the nonlinear polarization rotation in the SOA into account, the mode-locked pulses with peak power and pulse width are *0.16mW* and *6ps*, 0.56*mW* and *19.8ps* at a repetition rate of *2 GHz* respectively, can be obtained via the proposed model. The system stability is also enhanced greatly by the similar principle in [6]. We hope this work will be helpful to afford a deeper insight on the harmonic mode-locked fiber ring laser.

References

[1] Y. D. Gong, X. L. Tian, M. Tang, Opt. Commun. **265**, 628 (2005).

[2] S. Li, K. T. Chan, H. Ding, Z. Fang , Proc. Conf. Lasers Electo-Optics. **11**, 473 (1997).
[3] X. Feng, Y. Liu, H. Zhang, Microwave Opt. Technol. Lett. **44**, 196 (2005).
[4] Luis C. Archundia, Bojan Resan, Peter J. Delfyett, Appl. Phys. Lett. **85**, 4567 (2004).
[5] G. Y. Jiang, Z.M.Wu,G.Q.Xia, SPIE. **6020**, 599 (2005).
[6] J. He,K. T. Chan, Electronics Letters. **38**, 1504 (2002).
[7] C. G. Lee, Y. J. Kim, C. S. Park, IEEE/OSA J. Lightwave Technol.**24**, 1237 (2006).
[8] S. Diez, A. Mecozzi, J. Mørk,Opt. Lett. **24**, 1675 (1999).
[9] X.Yang, Z. Li, E. Tangdiongga, D. Lenstra, Opt. Exp. **12**, 2448 (2004).
[10] X. Yang, D. lenstra, G. D. Khoe, H. J. S. Dorren, Opt. Commun. **2**, 169 (2003).
[11] K. Zoiros,T. Stathopoulos,Opt.Commun. **180**, 301 (2000).
[12] G. P. Agrawal, Nonlinear Fiber Optics.2nd Edition, Academic Press, American (1995).

*Corresponding author: jgy579@126.com